



Optimum shape design of a BLDC motor for electric continuous variable valve timing system considering efficiency and torque characteristics

Soo-Whang Baek¹

Received: 12 November 2017 / Accepted: 6 June 2018 / Published online: 15 June 2018
© Springer-Verlag GmbH Germany, part of Springer Nature 2018

Abstract

Recently, environmental problems caused by global warming and exhaust gas have been increasing, leading governments all over the world to implement strict environmental regulations. For this reason, the automotive industry has begun working to increase fuel efficiency and reduce emissions. In addition, in order to improve the performance of engines implemented in internal combustion engines (ICEs) and hybrid electric vehicles (HEVs), electronic control actuators are becoming increasingly preferred over conventional mechanical parts. In particular, engine intake and exhaust valve timing techniques are critical to improving fuel economy and reducing vehicle emissions. Previously, a hydraulic continuous variable valve timing (CVVT) system was used for valve timing control. However, a disadvantage of this type of system is that the response speed is slow at low and high engine temperatures; these conditions limit the extent of automobile fuel efficiency improvement. Therefore, an electric variable valve timing system (E-CVVT) is being studied to overcome this disadvantage. In this paper, we propose a shape optimum design method for brushless DC (BLDC) motors used in an electric continuous variable valve timing (E-CVVT) system, which is employed in ICEs and HEVs. The proposed design aims to maximize the maximum torque and rated efficiency of BLDC motors, and minimize cogging torque. To select the optimal design variables, we chose to implement Latin hypercube sampling (LHS) to avoid duplication of sampling points. The characteristics of the sampling points obtained via the LHS method were calculated by using finite element (FE) analysis. In order to consider the nonlinearity of properties, we have created an approximate modeling technique that uses a radial basis function. Finally, genetic algorithms were used to determine the design parameters of the optimum model. The effectiveness of the proposed BLDC motor design process is verified by comparing the FE analysis and experimental results. Simulation and experimental results confirmed that the proposed optimized design procedure yields improved operating characteristics. Specifically, testing the proposed optimized design yielded a 16.7% increase in the maximum torque, and a 66.2% reduction in the cogging torque. In addition, the vehicle test confirmed that the proposed design was suitable for an E-CVVT system equipped with a BLDC motor. In addition, the optimum model of the BLDC motor was applied to the E-CVVT system. The response characteristics of the conventional hydraulic CVVT system and E-CVVT were compared via vehicle testing. The response speed of the E-CVVT system was 0.65 s faster than that of the CVVT system during the retard angle phase. Therefore, it was a 39.4% improvement in the response performance.

1 Introduction

The fuel efficiency, output, and emission performance of an automobile largely depend on the intake and exhaust timing of the engine. Even if the intake stroke is

completed, inertia acts on the air flowing into the cylinder. Therefore, the air in the cylinder is forcibly introduced into the cylinder, and the exhaust gas after combustion is not completely discharged from the engine. When the timing of the intake and exhaust valves is controlled at a low speed, the emission of the exhaust gas in the cylinder is delayed. Conversely, if the timing of the valve is controlled at a high speed, the compression stroke generated in the mixer of the engine is delayed, and the efficiency of the engine is substantially reduced. Consequently, pumping loss occurs in the cylinder of the engine, the fuel

✉ Soo-Whang Baek
swbaek@honam.ac.kr

¹ Department of Automotive Engineering, Honam University, 417 Eodeung-daero, Gwansan-gu, Gwangju 62399, Korea

consumption of the vehicle is reduced, and, due to inefficient driving conditions, unnecessary CO₂ and NO_x emissions increase. Therefore, it is necessary to improve the efficiency of intake and exhaust processing, and a technique to control the overlap section of intake and exhaust valves via variable valve timing is required (Dresner and Barkan 1989).

Variable valve timing (VVT) was developed because it requires that valve timing vary according to engine speed. VVT is a system that changes the valve opening/closing timing in two steps (low-speed and high-speed rotation of the engine). However, because the VVT system only operates under certain operating conditions (low/high speed), it cannot satisfy all the operating conditions of the engine (Grohn et al. 1989).

In order to overcome these problems, a method of continuously varying the valve timing has been developed into technology called continuous variable valve timing (CVVT) (Schäfer 2007). The purpose of the CVVT system is to improve torque reduction problems in low- and medium-speed regions, which reduce engine efficiency, and to improve fuel economy and reduce harmful emissions in the practical section (low- and medium-speed rpm). Conventional CVVT systems using hydraulic pressure are disadvantageous because the viscosity of the engine oil increases in the low-temperature and low-speed ranges, thereby making it difficult to quickly adjust the intake valve timing. Therefore, an electric CVVT (E-CVVT) system designed to maximize engine performance for all speed ranges has been proposed (Hattori et al. 2008).

Unlike conventional CVVT systems that use hydraulic pressure, the E-CVVT system uses motors to control intake valve timing. Because a motor is used, the structure is relatively simple, and the phase angle can be more precisely controlled. In particular, the response is significantly improved and the operating range can be improved under low-temperature conditions as compared to the CVVT systems using engine oil. This means that the E-CVVT system more accurately controls the timing than the CVVT system, improves fuel economy and engine output, and reduces exhaust gas. For these reasons, the use of motor systems is becoming increasingly referred to as a replacement for automobile hydraulic systems. The currently employed E-CVVT system is driven by a DC motor. However, because the durability and EMC characteristics of DC motors are degraded by brush, the E-CVVT system has been equipped with a BLDC motor to achieve high efficiency and reliability (Shrivastava et al. 2014).

In this paper, we propose an optimum shape design to improve the efficiency and maximum and cogging torque characteristics of the BLDC motor. To achieve an optimum design, the design parameters and range of the shape were selected as based on the mechanical dimensions of the

initial model. In a previous study, the optimum design of a single-phase line-start PM motor that considers the efficiency, maximum torque, and starting torque was studied, but there was a difference in the optimum design method of the AC motor used in the industrial fan, and the cogging torque of the motor was not considered (Baek et al. 2012). For the design of experiment (DOE), we apply the Latin hypercube sampling (LHS) technique (Shin et al. 2008; Kim et al. 2011), which provides the accuracy and reliability of sample points. Additionally, approximate modeling is performed by applying the radial basis function (RBF) (Yang et al. 2009; Bhuvanawari et al. 2005) to more accurately consider nonlinear characteristics. The search for the optimum design parameters is then performed by implementing a genetic algorithm (GA) (Upadhyay et al. 2005; Ahn et al. 2010). The characteristics of the optimum model obtained via the proposed optimum design process are calculated by using finite element (FE) analysis. Furthermore, the optimum model of a BLDC motor is fabricated as a prototype, and the validity of the proposed optimum design process is verified via dynamo testing. Finally, the optimum model of the BLDC motor is applied to the E-CVVT system, and the vehicle test is performed; the results are compared to the characteristics of the existing hydraulic CVVT system. Via this study, it is confirmed that the response speed of the cam phase angle of the E-CVVT system is improved as a result of implementing the optimum BLDC motor model as compared to that of the conventional hydraulic CVVT system.

2 E-CVVT system and BLDC motor

2.1 E-CVVT system

Figure 1 shows the general structure of the E-CVVT system. In the E-CVVT system, an engine control unit (ECU) in a vehicle receives the number of revolutions of the camshaft and the number of crank revolutions from the crankshaft from a sensor installed in the camshaft. The ECU calculates the current phase as based on the signal received from the sensors, and determines various command values needed to control the BLDC motor. The basic E-CVVT system comprises a chain system connected to a decelerator, which is connected to a camshaft and a timing system for engine power transmission, a sensor capable of measuring current time, and an actuator to vary the cam phase. The actuator uses a BLDC motor with high reliability and fast response characteristics.

The main components of the E-CVVT consist of a BLDC motor, cycloid reducer, and motor controller, as is shown in Fig. 2. The ECU sends the appropriate command

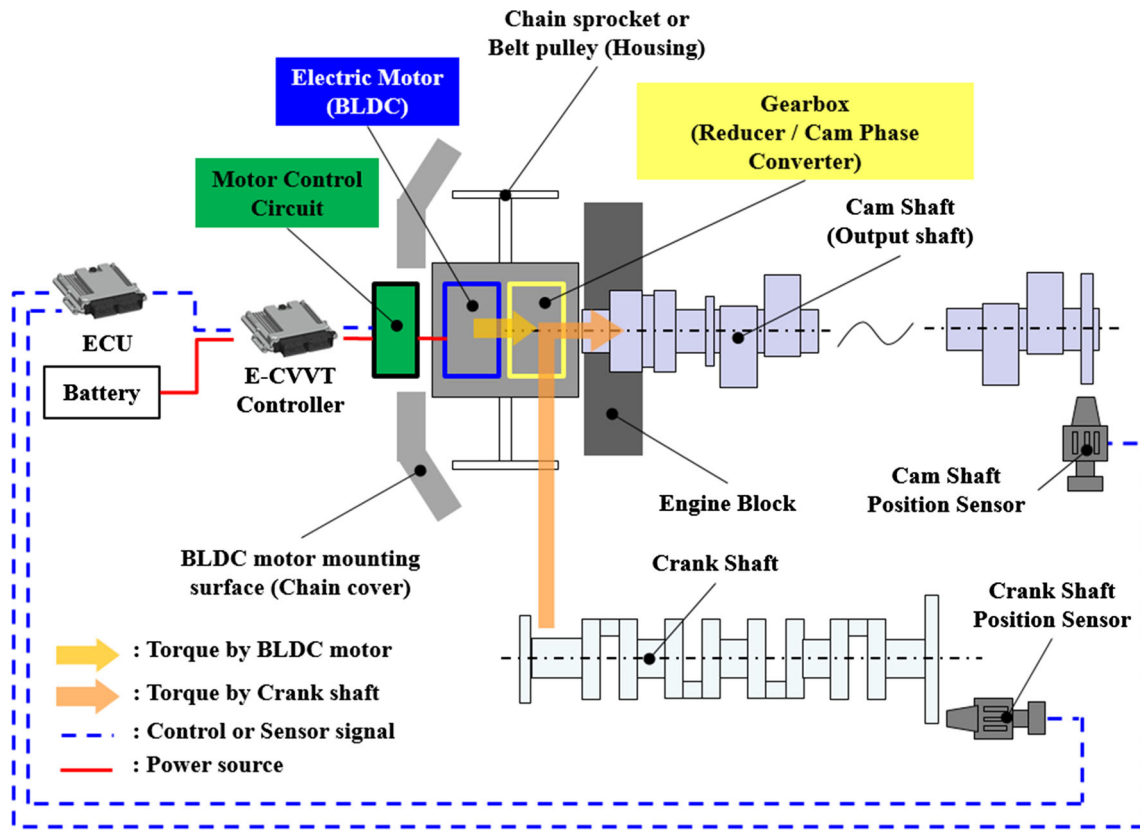


Fig. 1 General structure of E-CVVT system

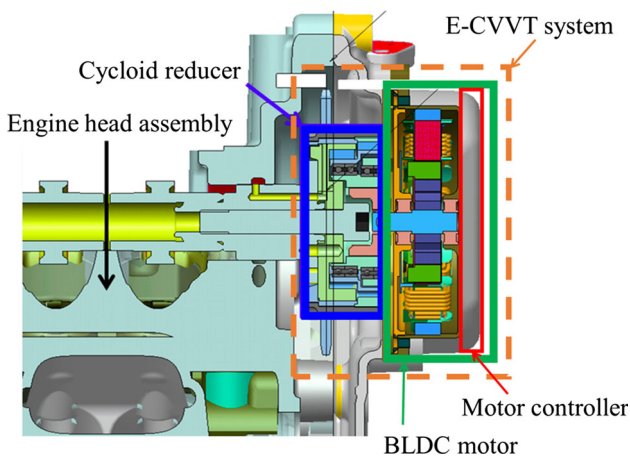


Fig. 2 Structure of E-CVVT

to the motor controller, as according to the operating conditions, via controller area network (CAN) communication. The motor controller determines the rotor position of the motor and turns on the power supply to initiate rotation of the BLDC motor. The shaft of the BLDC motor allows the BLDC motor and cycloid reducer to be assembled as a combined structure. The output torque of the BLDC motor is amplified by using a cycloid reducer with a high reduction gear ratio (100:1), which can overcome the

large load of the intake camshaft and drive the E-CVVT. With this method, the intake valve timing is adjusted according to the operating conditions via the closed loop control initiated by the ECU to optimize valve timing.

Figure 3 compares the intake and exhaust valve timing, showing that the phase of the camshaft is altered by the rotation of the BLDC motor, and that the angle of the valve

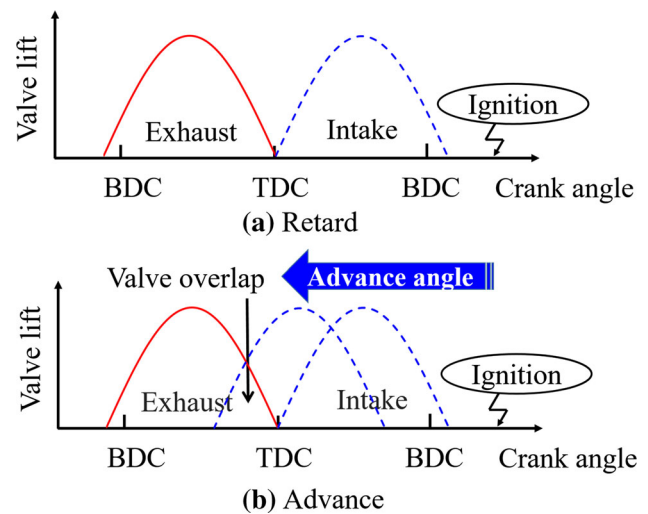


Fig. 3 Comparison of camshaft phase according to valve timing

timing is advanced and retarded. In this figure, TDC is the top dead center and BDC refers to the bottom dead center.

The BLDC motor is used to rotate with the intake camshaft and adjust valve timing when the engine is running. There are three E-CVVT operating modes. First, to maintain valve timing, the BLDC motor operates at the same speed as the camshaft. Second, the BLDC motor rotates slightly faster than the camshaft speed to advance valve timing. Third, to retard valve timing, the BLDC motor rotates at a slightly slower speed than the camshaft speed. The advantages of implementing E-CVVT with a BLDC motor are excellent response and accuracy at low engine speeds and temperatures.

2.2 BLDC motor for E-CVVT

The BLDC motor is constructed with brushes and commutators removed, yielding EMC characteristics that are superior to DC motors. For this reason, BLDC motors have the advantage of being suitable for use in automotive applications. In this study, a BLDC motor with excellent response and reliability is optimized to drive the E-CVVT. Figure 4 shows the assembly and a cross section of the BLDC motor. Table 1 shows the specification of BLDC motor that satisfy the performance requirements and has a suitable engine layout. The BLDC motor is driven via a six-step rectangular wave 120-degree switching method. The response performance of the E-CVVT system driven by the BLDC motor is proportional to the magnitude of the maximum torque of the BLDC motor, and the lower the torque ripple and cogging torque characteristics of the BLDC motor, the better the stability of control. Therefore, in this paper, as an approach to improve the response performance and control stability of the E-CVVT system as mentioned above, we performed the optimum shape design

Table 1 Specification of BLDC motor

System parameters	Unit	Values
Rated voltage	V	13.5
Rated output power	W	110
Rated torque	Nm	0.35
Rated speed	rpm	3000
Rated efficiency	%	88
Maximum speed	rpm	5000
Maximum torque	Nm	1.2
Cogging torque (peak to peak)	Nm	0.238
Outer diameter of rotor	mm	48
Stack length	mm	10
Number of slot	Slots	12
Diameter of coil	mm	0.7
Number of turns	Turns	15
Number of pole	Pole	14
Permanent magnet	–	N42UH
Length of air-gap	mm	0.5

of the BLDC motor and confirmed the improvement of the performance of the BLDC motor.

3 Optimum design

The proposed optimum design considers the efficiency, maximum torque, and cogging torque of a BLDC motor. The process of optimum the motor design is illustrated in Fig. 5. According to this optimum design, the mechanical dimensions of the stator and rotor—i.e., the diameter and stack length of cores—are fixed. If the outer diameter of the stator is changed, the outer diameter of the rotor is also changed, thereby changing the capacity of the motor. Therefore, the optimum design result cannot be correctly obtained because the criteria that can be directly compared to the characteristics of the initial model become unclear. If the thickness of the stator yoke is selected to be thin, the thickness of the stator yoke is designed in order to prevent the core from being magnetically saturated. For this reason, the thickness of the stator yoke is not selected as a design parameter in order to design the optimum model under the same output conditions. In addition, when the outer diameter of the rotor and the length of the lamination are determined by the design parameters, the mechanical structure of the motor is changed to a size that cannot be mounted onto the E-CVVT system. Therefore, the range of the optimum design parameters was appropriately selected to maintain the rated output of 110 W.

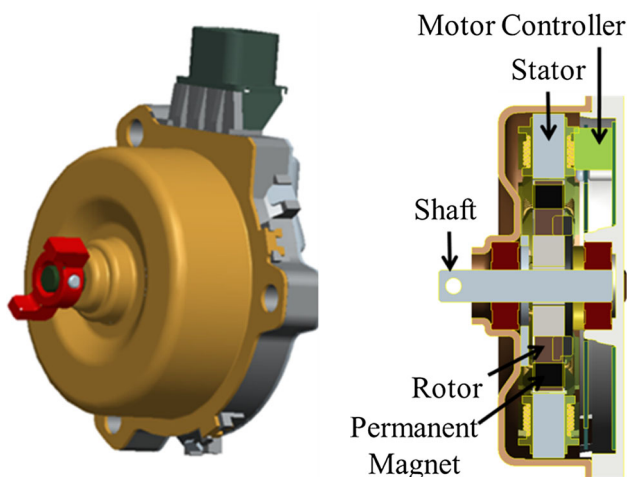


Fig. 4 Structure of BLDC motor

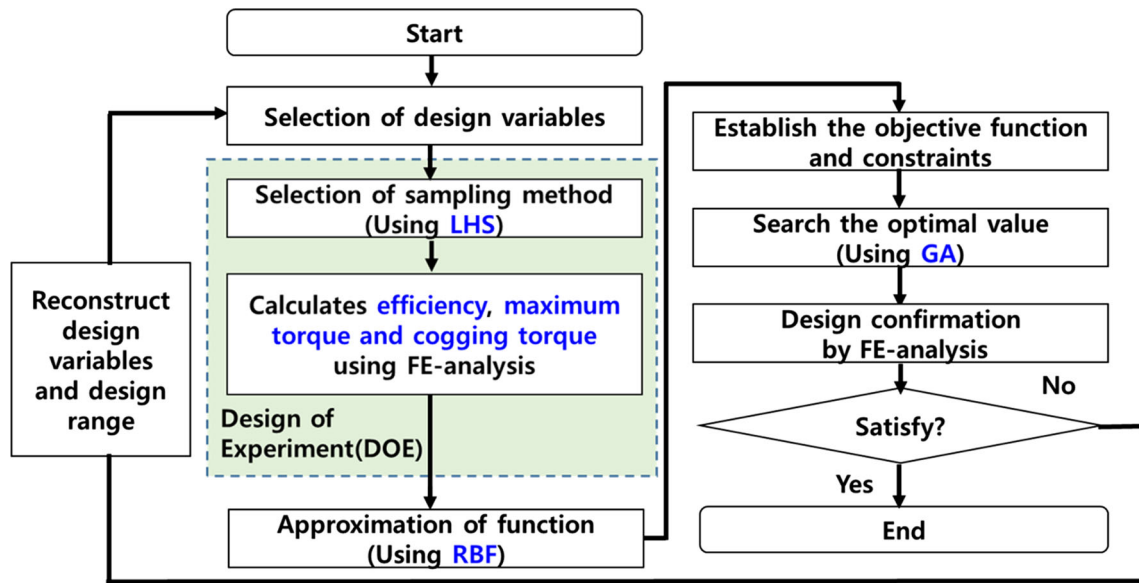


Fig. 5 Proposed optimum design process

The DOE determines the optimum design variables and range of these variables; moreover, it is a way to plan how to best perform experiments in order to solve the representative problems and obtain valid information while also minimizing the number of required experiments. The first step in the DOE entailed selecting the design variables for the optimum design. Figure 6 shows the design variables. The slot opening (X1) was chosen as a design variable to reduce leakage flux and increase efficiency, whereas eccentricity (X2) was chosen to reduce the cogging torque by maintaining a constant air gap. Lastly, the center of the hole (X3) was determined such that it increased the maximum torque by reducing the leakage flux of the rotor. Generally, these design variables were chosen to optimize the system design because they affect the efficiency, maximum torque, and cogging torque of BLDC motors.

The ranges of the design variables considered to optimize the system design are shown in Table 2.

For the range of the slot opening (X1), the minimum value is twice the coil diameter ($0.7 \times 2 = 1.4$ mm), and the maximum value is that of the initial model (4 mm). As presented above, the eccentricity (X2) ranges from the minimum value of 0 mm, to the maximum value of 2.0 mm; the center of hole (X3) ranges from the minimum value of 5 mm, to the maximum value of 15 mm. This is a limiting value in manufacturing. LHS was used to select the sampling point. LHS is the first step in optimum design variables and their respective ranges. It is the process of searching for many design variables in order to satisfy the optimum design condition. Table 3 shows the distribution of samples resulting from LHS. During acquisition of the sampling points, all duplicated samples were removed; the results are shown in Fig. 7. Considering the number of

Fig. 6 Design variables

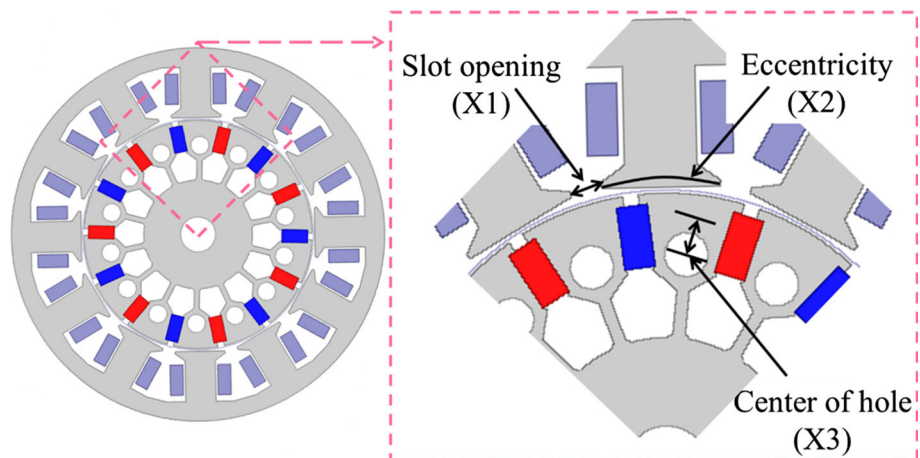


Table 2 The ranges of the design variables

Variable	Lower	Upper	Unit	Remark
X1	1.4	4	mm	Slot opening
X2	0	2.0	mm	Eccentricity
X3	5	15	mm	Center of hole

Table 3 Sample distribution using LHS

Sample	Design variables		
	X1	X2	X3
1	1.9	0.4	11.4
2	1.6	0.5	10.3
3	2.7	0.7	6.3
4	2.1	1.6	8.2
5	2.0	0.3	9.3
6	2.8	1.2	7.8
7	3.8	0.6	12.4
8	1.4	1.5	11.8
9	3.2	0.9	14.5
10	1.7	1.3	5.7
11	3.4	1.7	13.4
12	3.9	0.8	9.2
13	3.7	0.2	11.5
14	1.2	1.1	6.7
15	3.0	0.1	9.8
16	2.4	0.8	13.0
17	2.9	1.9	12.1
18	2.3	1.3	14.0
19	3.5	1.8	6.9
20	1.5	2.0	14.2

design variables, the total number of sampling points in this experimental design (DOE) was 20. The sample points (X1, X2, and X3) are shown in two dimensions, and all three variables were selected such that there were no overlapping points. The efficiency, maximum torque, and cogging torque characteristics of the samples selected by LHS were calculated via FE analysis, and are provided in Table 4.

The data were interpolated from the characteristics listed in Table 4, and the approximation modeling was performed as based on a RBF in order to improve the accuracy of the optimized results. The objective functions and constraints were defined as shown below. The objective functions to maximize the maximum torque and rated efficiency and minimize the cogging torque were achieved by assigning the same weight to each objective function. The constraints were set such that the maximum torque exceeded 0.12 Nm and the peak-to-peak of the cogging torque was less than 0.065 Nm of the initial model.

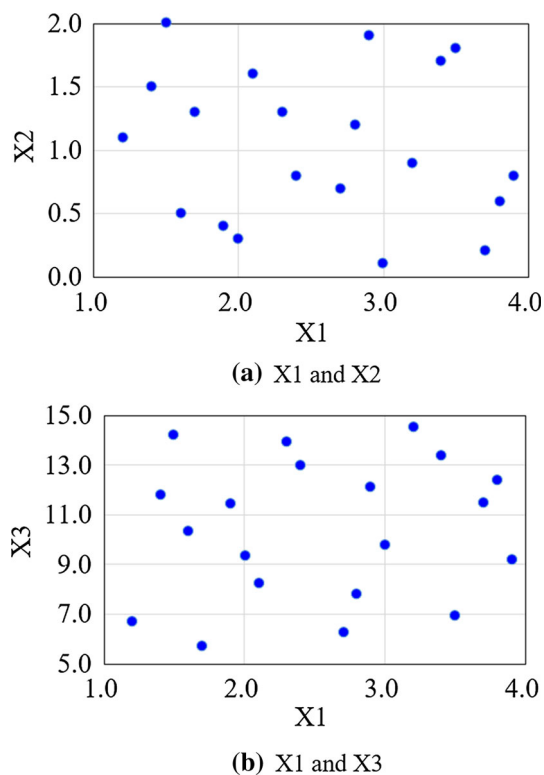


Fig. 7 LHS results: sample distribution map

1. Objective functions:

- (a) Maximize torque and rated efficiency.
- (b) Minimize cogging torque.

2. Constraints:

- (a) Maximum torque > 0.12 Nm.
- (b) Cogging torque < 0.065 Nm (peak to peak).

Equation (1) below was used to calculate the torque characteristics (Hendershot and Miller 2010):

$$T = \frac{1}{\mu_0} \int_0^{2\pi} r^2 B_r \cdot B_t d\theta \quad (\text{Nm}) \tag{1}$$

where T is the electromagnetic torque, B_r is the radial component of air gap flux density, B_t is the tangential component of air gap flux density, and μ_0 is the permeability of an air gap.

The cogging torque, which is a force acting in the direction in which the reluctance is minimized, is expressed as Eq. (2) (Gieras et al. 2004).

$$T_{cog} = -\frac{1}{2} \phi_g^2 \frac{dR}{d\theta_r} \tag{2}$$

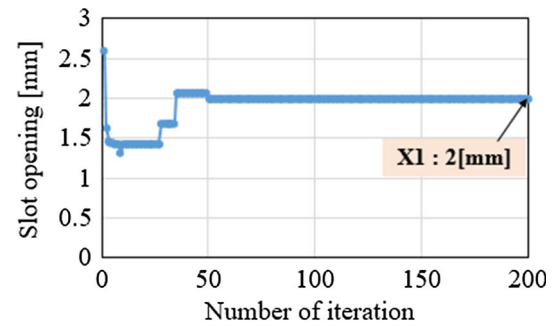
where ϕ_g is the flux of an air gap, R is the reluctance of air gap flux density, and θ_r is the rotating angle.

Table 4 Characteristics of sample obtained from LHS using FE-analysis

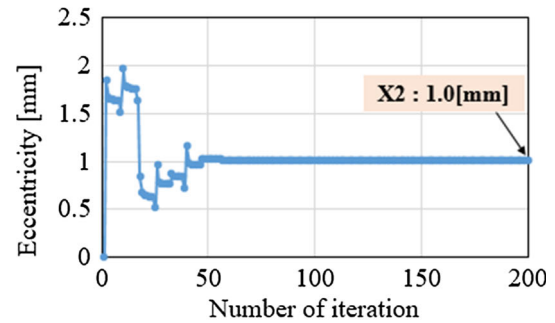
Sample	Efficiency (%)	Maximum torque (Nm)	Cogging torque (Nm)
1	88.10	1.400	0.067
2	88.25	1.360	0.060
3	87.02	1.180	0.045
4	87.90	1.240	0.049
5	87.30	1.250	0.040
6	86.76	1.220	0.062
7	85.35	1.380	0.053
8	88.11	1.150	0.061
9	86.17	1.270	0.026
10	88.18	1.050	0.069
11	85.90	1.290	0.058
12	88.13	1.280	0.065
13	85.62	1.370	0.034
14	88.27	1.070	0.043
15	86.43	1.100	0.028
16	87.60	1.350	0.056
17	86.81	1.410	0.048
18	87.82	1.280	0.050
19	85.70	1.090	0.037
20	88.25	1.310	0.024

A GA was developed to investigate the optimum design variables by using approximate models. The GA was used to determine the optimum design variables as based on the above-listed objective functions and constraints set for the optimum design. The characteristics of the maximum torque and cogging torque were set as constraints such that the operating characteristic will not be lower than that of the initial model. Additionally, if the optimum design result converged to the desired target, optimization was concluded; otherwise, the optimum design variables were adjusted until convergence to the desired design result was achieved within the given constraint. Figure 8 shows the respective 200-iteration convergence profiles of each of the three design variables investigated in this study. The convergence resulted in the design variables being adjusted for optimal efficiency, maximum torque, and cogging torque.

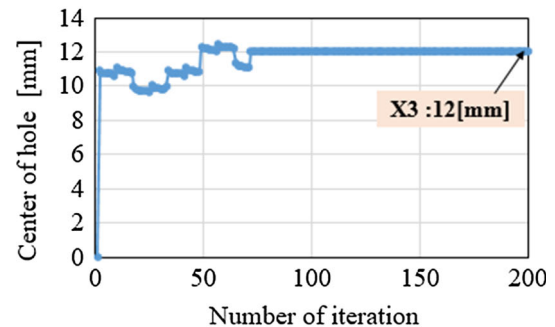
Table 5 compares the values of the initial and optimum model design variables. The shape of the optimum model was determined by the proposed optimum design process. Figure 9 illustrates the comparison between the initial model and optimum model.



(a) Slot opening (X1)



(b) Eccentricity (X2)



(c) Center of hole (X3)

Fig. 8 Convergence profile of design variables

4 Verification of simulation and experiment

4.1 Simulation results

FE analysis was used to validate the characteristics of the optimum design model. The 2D FE analysis by using the commercial software, ANSYS-Electromagnetics Suite 18.0, was utilized to predict the motor characteristics. To ensure the analysis accuracy, a high quality mesh with 80,000

Table 5 Comparison of design variables

Variable	Initial	Optimum	Unit
X1	2.6	2.0	mm
X2	0	10	mm
X3	0	12	mm

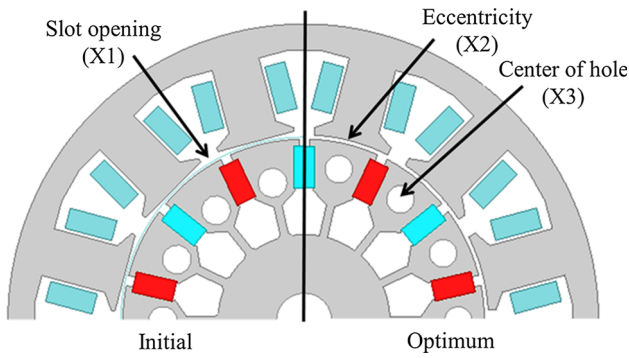


Fig. 9 Comparison of initial and optimum models

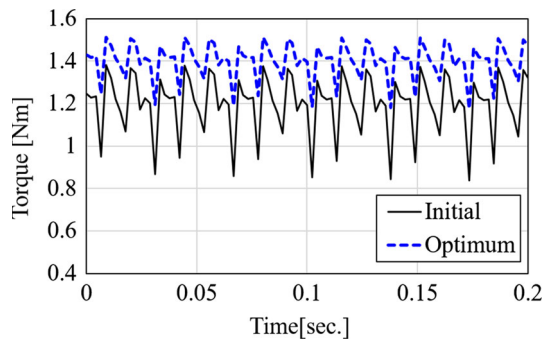


Fig. 10 Comparison of the maximum torque characteristics (FE analysis)

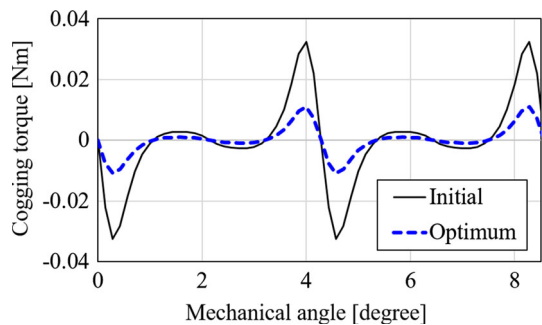


Fig. 11 Comparison of the cogging torque characteristics (FE analysis)

elements and 51,000 nodes of the BLDC motor was utilized for torque performance prediction. For the simulation analysis, three-phase six-step rectangular wave 120° current was applied to stator winding. The input voltage was 13.5 V. The end turn effects of the windings were considered by including the parameter in an external circuit. The characteristics of maximum torque and cogging torque are compared in Figs. 10 and 11, respectively. The comparison of the maximum torque characteristics in Fig. 10 means that the torque ripple characteristic at the maximum torque condition that the motor can generate is calculated. Here, the stability of the E-CVVT system is improved by reducing the difference in the torque ripple peak value. Figure 11 compares the

Table 6 Comparison of the operating characteristics (FE analysis)

Items	Initial	Optimum	Unit	Remarks
Rated efficiency	88.0	88.0	%	Maintain
Maximum torque	0.12	0.14	Nm	Increase 16.7%
Cogging torque	0.0650	0.0205	Nm	Decrease 68.5%

cogging torque characteristics caused by the reluctance difference in the circumferential direction of the air gap. To reduce the cogging torque, the difference in reluctance must be minimized. When the cogging torque is reduced, the normal force is also reduced and the vibration and noise characteristics are improved.

Table 6 compares the operating characteristics of the initial model and optimum model. The simulation results show that the rated efficiency, which is relative to the level of the initial model, was maintained at a level of 88.0%, whereas the maximum torque increased by 16.7% from 0.12 (initial model) to 0.14 Nm (optimum model). Additionally, the optimum model yielded a cogging torque that was reduced by 68.5% (0.0205 Nm) relative to the 0.0650-Nm value of the initial model. Thus, from the perspective of the maximum torque and cogging torque, the proposed optimum model is better than the initial model.

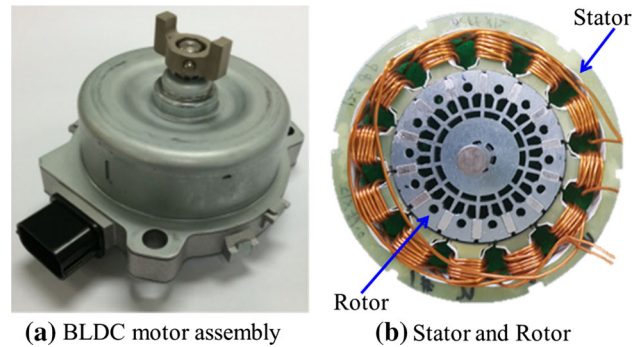


Fig. 12 Optimum BLDC motor prototype

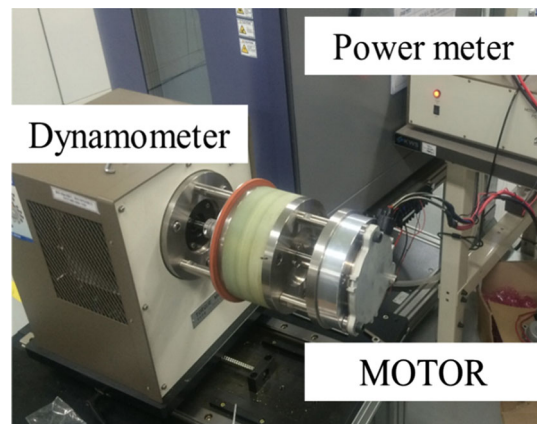
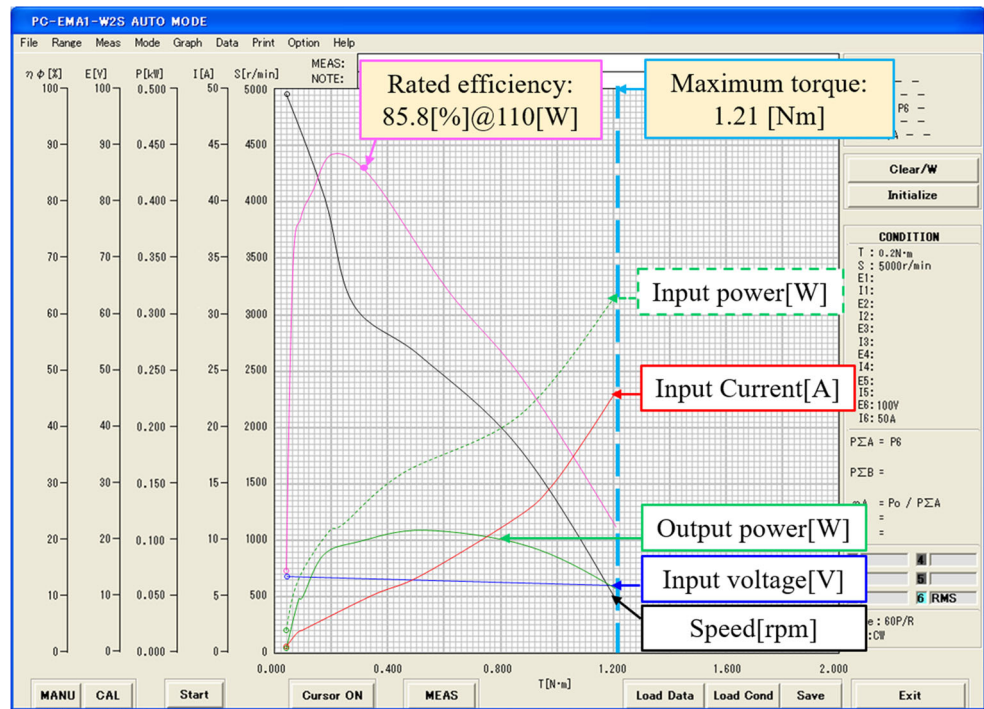
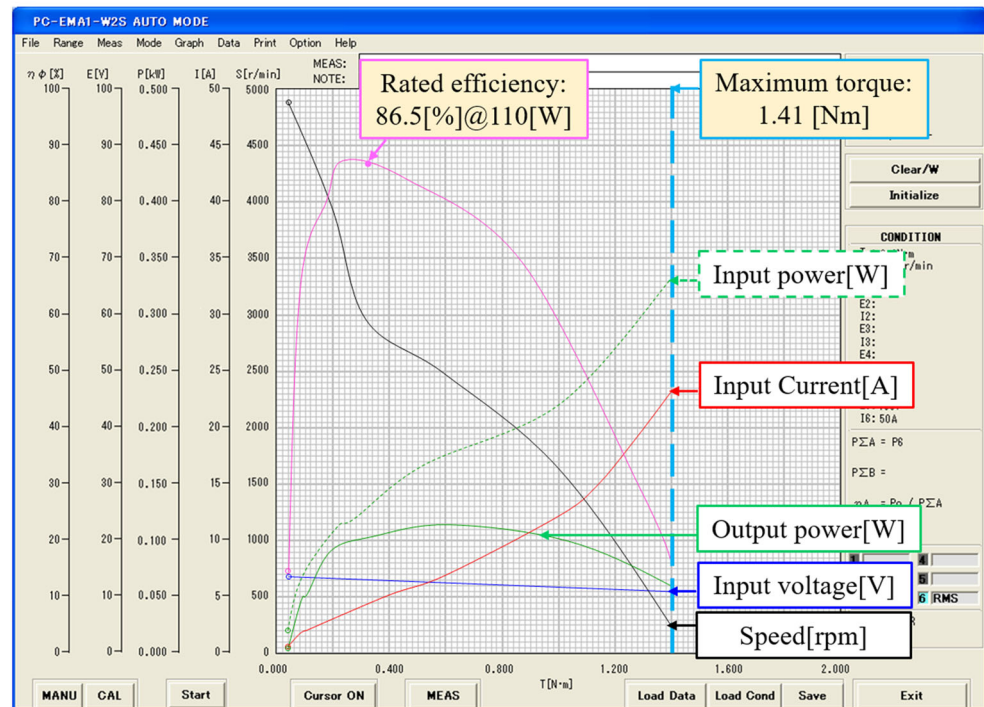


Fig. 13 Experimental setup for motor dynamo testing (experiment)

Fig. 14 Comparison of motor dynamo test results (experiment)



(a) Initial model



(b) Optimum model

4.2 Experimental results

To verify the proposed optimum design process, a prototype of the optimum BLDC motor was fabricated. The prototype BLDC motor assembly, stator, and rotor are

shown in Fig. 12, and the experimental setup is illustrated in Fig. 13. The measurement targets were the current, speed, and the efficiency and torque characteristics as a function of the speed. The input voltage was 13.5 V.

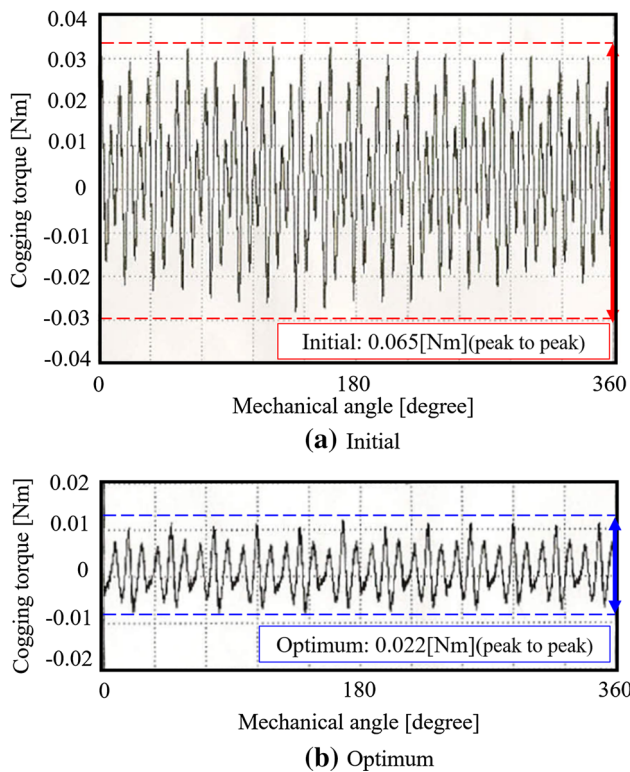


Fig. 15 Comparison of cogging torque characteristics (experiment)

Table 7 Comparison of the operating characteristics (experiment)

Items	Initial	Optimum	Unit	Remarks
Rated efficiency	86.5	86.3	%	Decrease 0.2%
Maximum torque	1.21	1.41	Nm	Increase 16.5%
Cogging torque	0.065	0.022	Nm	Decrease 66.2%

The experimental results of motor dynamo testing are presented in Fig. 14. The performances were tested using prototype motors.

To compare the operating characteristics, the BLDC motor was started at a no-load speed of 5000 rpm, and the load torque was continuously increased during the experiment. The maximum torque results demonstrate that the initial and optimum models exhibit reduced rotation at a load torque of 1.12 and 1.41 Nm, respectively. Furthermore, it is clear that the experimental results are in agreement with the analysis results illustrated in Fig. 10, as the maximum torque of the initial model was higher than that of the initial model. However, at 3000 rpm, the rated efficiency of the initial model was 86.5%, whereas that of the optimum model was 86.3%. This indicates that the rated efficiency characteristics of the initial model and optimum model are similar. The reason that the rated efficiency of the test results yields an approximately 1.5%



Fig. 16 Vehicle test setup

Table 8 Vehicle test condition

Items	Initial	Unit
Input voltage	13.5	V
Current limit	25	A
Engine speed	1000	rpm
Cam shaft speed	500	rpm
Variable range of cam phase angle	0–24	Degree
Ambient temperature	25	°C

reduction relative to the results of the analysis is considered to be due to the inclusion of mechanical and friction loss.

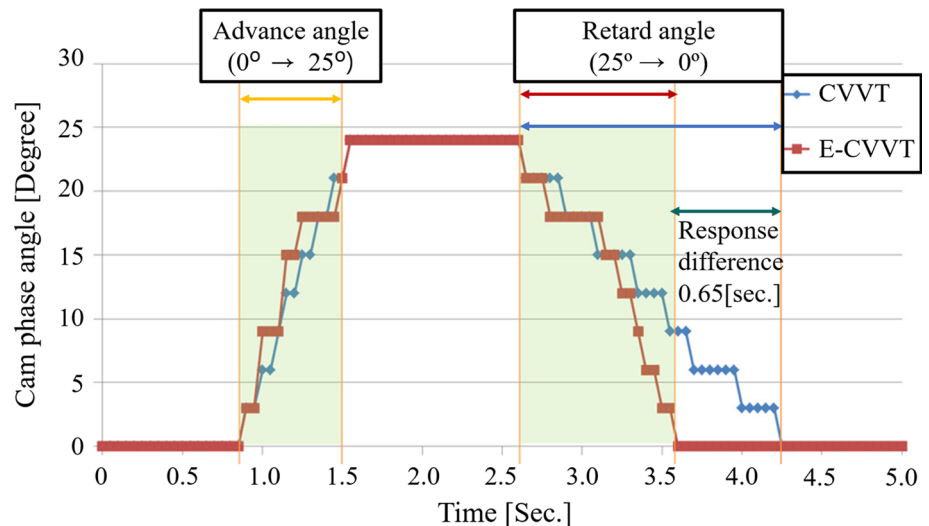
A comparison of the cogging torque characteristics are shown in Fig. 15. The initial model yielded a cogging torque of 0.065 Nm, whereas that of the optimum model was 0.022 Nm; this reduction is due to the reduced magnetic reluctance difference between the rotor magnet and stator slots. The experimental operating characteristics of the initial and optimum models are shown in Table 7. These results indicate that the proposed optimum design process may be very useful for the design of a BLDC motor.

4.3 Vehicle testing results

Finally, a vehicle test was performed to compare the performance of a hydraulic CVVT system and an E-CVVT system controlled by a BLDC motor. Figure 16 shows the vehicle test setup; the optimum model for the BLDC motor in Fig. 12 was installed in the E-CVVT system. The comparison target was the response speed of the cam phase angle for valve timing control; the vehicle testing conditions are presented in Table 8.

The response speed results for the CVVT and E-CVVT system cam phase angles are respectively shown in Fig. 17. There was no significant difference between the response speeds of each cam phase angle during the advance angle phase. In contrast, the response speed of the E-CVVT

Fig. 17 Comparison of cam phase angle response (experiment)



system was 0.65 s faster than that of the CVVT system during the retard angle phase. As a result, there was a 39.4% improvement in the response performance. For reference, the temperature condition for this vehicle test was 25 °C. At low temperatures, the response speed of the CVVT is reduced because the viscosity of the engine oil increases. Therefore, it is expected that the response speed of the E-CVVT and BLDC motor system will be improved and will contribute to the improvement of the fuel efficiency of vehicles.

5 Conclusion

This paper has proposed an optimum design that considers the efficiency and maximum and cogging torques of a BLDC motor in the development of an E-CVVT system. The design parameters and range of shape were selected for the proposed optimum design process. As a result, the rated efficiency of the BLDC motor was maintained at the level of the initial model, and the maximum torque of the BLDC motor was increased to improve the ability of the motor to withstand disturbances such as sudden large loads. Because a reduced cogging torque of the BLDC motor would result in a reduced torque ripple and improved control performance, we tried to reduce this design parameter. Simulation and experimental results confirmed that the proposed optimum design procedure yields improved operating characteristics. Specifically, testing the proposed optimum design yielded a 16.7% increase in the maximum torque, and a 66.2% reduction in the cogging torque. In addition, the vehicle test confirmed that the proposed design was suitable for an E-CVVT system equipped with a BLDC motor. The BLDC motor-based optimum design method developed in this study is expected to be extended to

achieve a comprehensive optimized motor design to drive an electric oil pump and electric water pump to improve automobile fuel efficiency.

The limitation of this study is that the design parameters related to stator coils and permanent magnet shapes are excluded as design parameters. By changing the slot area of the stator of the BLDC motor to increase the turn number of the coil and increase the amount of the permanent magnet, the characteristics of the BLDC motor can be improved. In future research, it is necessary to optimize the PID parameters to improve the BLDC motor control characteristics, and further improve the response speed and controllability of the E-CVVT system.

Acknowledgements This paper was supported by the National Research Foundation of Korea (NRF) grant funded by the Korea Government (MSIT) (no. 2017R1C1B5075525); this study was also supported by a 2017 research fund from Honam University.

References

- Ahn Y et al (2010) Novel memetic algorithm implemented with GA (genetic algorithm) and MADS (mesh adaptive direct search) for optimal design of electromagnetic system. *IEEE Trans Magn* 46(6):1982–1985
- Baek SW et al (2012) Optimum design of a single-phase line-start PM motor considering efficiency, maximum torque, and starting torque. *IEEE Trans Magn* 48(12):4850–4859
- Bhuvanewari R et al (2005) Optimization of single-phase induction motor design using radial basis function network. In: *INDICON 2005 annual IEEE*. <https://doi.org/10.1109/indcon.2005.1590119>
- Dresner T, Barkan P (1989) A review of variable valve timing benefits and modes of operation. *SAE Technical Paper* 891676. <https://doi.org/10.4271/891676>
- Gieras JF, Wang RJ, Kamper MJ (2004) *Axial flux permanent magnet brushless machines*. Kluwer Academic Publishers, Dordrecht, pp 37–41

- Grohn M et al (1989) Variable valve timing in the New Mercedes-Benz four-valve engines. In: SAE technical paper 891990. <https://doi.org/10.4271/891990>
- Hattori M et al (2008) Development of variable valve timing system controlled by electric motor. SAE Int J Engines 1(1):985–990
- Hendershot JR Jr, Miller TJE (2010) Design of brushless permanent-magnet motors. Motor Design Books, Venice, pp 107–108
- Kim JB et al (2011) Optimization of two-phase in-wheel IPMSM for wide speed range by using the kriging model based on Latin hypercube sampling. IEEE Trans Magn 47(5):1078–1081
- Schäfer J et al (2007) High performance electric camshaft phasing system. In: SAE technical paper 2007-01-1294. <https://doi.org/10.4271/2007-01-1294>
- Shin P-S et al (2008) An application of Latin hypercube sampling strategy for cogging torque reduction of large-scale permanent magnet motor. IEEE Trans Magn 44(11):4421–4424
- Shrivastava N et al (2014) Design of 3-phase BLDC motor for electric vehicle application by using finite element simulation. Int J Emerg Technol Adv Eng 4(1):140–145
- Upadhyay PR et al (2005) Genetic algorithm based design optimization of a permanent magnet brushless dc motor. J Appl Phys 97:10Q516. <https://doi.org/10.1063/1.1860891>
- Yang G et al (2009) A novel superposition RBF collocation method to solve moving conductor Eddy current problems. IEEE Trans Magn 45(10):3977–3980

Publisher's Note Springer Nature remains neutral with regard to jurisdictional claims in published maps and institutional affiliations.